J. Appl. Comput. Mech., xx(x) (2025) 1-11
DOI: 10.22055/jacm.2025.48637.5384

ISSN: 2383-4536
jacm.scu.ac.ir

Shahid Chamran University of Ahvaz

Journal of Applied and Computational Mechanics

Research Paper

Fault Detection in Wind Turbine Using Time-Domain Vibration Features and LOOCV-Tuned Neural Networks

Abdulhamid Hamdan Al-Hinai, Karu Clement Varaprasad, Viswanadhan Vinod Kumar

Department of Mechanical and Mechatronic Engineering, Sohar University, Sohar, Oman,
Email: abdulhamidalhinai@gmail.com (A.H.A.H.); CKaru@su.edu.om (K.C.V.); VKumar@su.edu.om (V.V.K.)

Received July 26 2025; Revised November 04 2025; Accepted for publication November 27 2025.
✉ Corresponding author: A.H. Al-Hinai (abdulhamidalhinai@gmail.com)

Abstract. This study proposes a novel, hardware-efficient condition monitoring approach for wind turbines using only time-domain vibration features and Leave-One-Out Cross-Validation with Artificial Neural Networks. Vibration data were collected from a lab-scale Wind Turbine Simulator under four conditions: healthy, bearing fault, blade crack, and blade imbalance, using sensors mounted on three orthogonal axes and acquired via NI 9234 DAQ. Statistical features like RMS, peak acceleration, crest factor, and shock pulse count were extracted and used to train a feedforward Artificial Neural Network. The horizontal-east axis provides the most diagnostic data and the model achieved 83.3% Leave-One-Out Cross-Validation accuracy with perfect recall for healthy and blade crack cases. This efficient approach enables scalable, real-time fault classification for intelligent wind energy systems.

Keywords: Artificial Neural Network, Fault Classification, Shock Pulse Detection, Time-Domain Vibration Analysis, Wind Turbine Condition Monitoring.

1. Introduction

The global transition to sustainable energy systems has positioned wind power as one of the most promising renewable energy sources [1]. Its scalability, cost-effectiveness and near-zero carbon emissions make the wind energy as a cornerstone of future power grids [2]. As the deployment of wind farms accelerates, particularly in offshore and remote environments, the reliability and maintainability of wind turbine systems became increasingly critical. The modern wind turbines are complex electromechanical systems comprising rotating blades, shafts, gearboxes, bearings, and generators operating under dynamic environmental conditions [3-5]. These wind turbine components are subjected to cyclic loading, fatigue, misalignment and other mechanical stresses that lead to progressive degradation or sudden failure. Therefore, the need for robust condition monitoring systems (CMS) is more pressing that can detect faults at an early stage and prevent catastrophic costly breakdowns [6-11].

Among the various techniques adopted in condition monitoring, the vibration analysis (VA) emerged as a dominant approach for identifying mechanical faults in rotating machinery [12]. The vibration signals encapsulate a wealth of information regarding the structural integrity and operational behaviour of the wind turbine components [13]. When processed effectively, these signals can reveal subtle changes in system dynamics. This can lead to a visible damage and failure. The conventional vibration analysis methods are typically classified into three domains: time-domain, frequency-domain and time-frequency-domain. Each of these domains gives a unique strength. However, the time-domain analysis remains particularly appealing due to its simplicity, computational efficiency and suitability for real-time and embedded applications [14].

The motivation to explore time-domain analysis as a standalone method stems from practical constraints encountered in field-deployable monitoring systems. Many CMS implementations face limitations in processing power, memory capacity and power consumption [15]. This is particularly with CMSs integrated into microcontroller-based or edge computing platforms. The Time-domain features, such as Root Mean Square (RMS), peak acceleration, crest factor and shock pulse count, can be computed with minimal resource overhead. This makes them ideal for embedded diagnostic systems [16]. These features also offer physical interpretability and enable maintenance decisions without requiring complex transforms or spectral analysis.

Numerous studies explored the use of vibration analysis in wind turbine fault detection, often leveraging advanced signal processing and machine learning techniques. For instance, Hasan et al. [17] investigated hybrid feature sets combining time-domain, frequency-domain and statistical entropy measures to detect faults in turbine gearboxes. Their results showed improved fault classification accuracy but underscored the increased computational burden. Similarly, Parziale et al. [18] and Kulevome et al. [19] integrated vibration and temperature signals using convolutional neural networks (CNN). They achieved a strong classification but required high-end Graphics Processing Units for real-time execution. These approaches, although valuable in offline diagnosis, face limitations in deployment on low-power edge devices. In contrast, Moghadam and Kakhki [20] explored statistical time-domain features for bearing fault classification using decision trees. They reported promising results with significantly lower computational

Published online: December 03 2025

requirements. Their study emphasized the diagnostic relevance of features like RMS, skewness and kurtosis. Al-Saad et al. [21] and Alzghoul et al. [22] further demonstrated that time-domain features could be successfully used in conjunction with artificial neural networks (ANN) to classify faults in small-scale rotating machinery. However, most existing research focuses on hybrid methods or combines multiple signal modalities. This leaves a gap in understanding the diagnostic power of time-domain features alone, particularly in the context of wind turbine simulators. Furthermore, few studies assess the comparative value of different sensor orientations (for example, vertical versus horizontal placement) in contributing to fault sensitivity.

Despite the advancements in vibration-based CMS, there remains significant research in systematic studies that focus exclusively on time-domain features without resorting to frequency or time-frequency transformations. This includes utilizing lab-scale wind turbine simulators to replicate realistic operational conditions, conducting comparative analyses of accelerometer orientations to optimize fault detection, assessing classifier performance using strong cross-validation strategies on minimal datasets and implementing lightweight, interpretable and embedded-ready diagnostic pipelines based solely on the time-domain metrics and machine learning. The present study investigates the standalone effectiveness of time-domain vibration analysis for fault detection in a lab-scale Wind Turbine Simulator (WTS). Specifically, it evaluates whether simple statistical features derived directly from accelerometer signals can accurately classify different operational states using an ANN model and identifies the most diagnostically informative accelerometer orientation among Horizontal East (HE), Horizontal West (HW) and Vertical (V) placements. The novelty and main contributions of this study involve feature engineering from Time-Domain analysis, multi-axis accelerometer assessment, lightweight ANN-based classification and validation with Leave-One-Out Cross Validation (LOOCV) technique.

2. Methodology

This section outlines the systematic methodology employed to implement time-domain vibration analysis for condition monitoring of a lab-scale WTS. Fig. 1 shows the WTS experimental setup layout while Fig. 2 shows the experimental flow chart for Time-Domain vibration analysis. Figure 1 illustrates the schematic configuration of the AI-based condition monitoring framework for a wind turbine simulator with a defective blade. The vibration data acquired through the NI 9234 DAQ and LabVIEW undergo time-domain analysis, ANN classification and Leave-One-Out Cross Validation. The approach is to combine experimental data acquisition, signal preprocessing, time-domain feature extraction and machine learning-based fault classification. This is to ensure the reproducibility, computational efficiency and suitability for real-time embedded systems.

The vibration signals and rotational speed data were collected using the National Instruments (NI) 9234 Data Acquisition (DAQ) module. The DAQ was configured with a sampling rate of 10,000 samples per second per channel. This is sufficient to capture the dynamic behaviour of mechanical faults in the wind turbine system. The NI 9234 is known for its high-resolution 24-bit analogue inputs and anti-aliasing filters. It provided a high-fidelity capture of transient and steady-state vibrations. The three uniaxial accelerometers were mounted on the secondary bearing block of the WTS in three orthogonal directions, namely: Horizontal East (HE), Horizontal West (HW) and Vertical (V), as shown in Fig. 3. These positions, also listed in Table 1, were selected to ensure multi-axis monitoring and to maximize the ability to detect directional fault symptoms such as blade imbalance and cracks. Additionally, a tachometer was integrated to monitor the shaft rotation in real-time. This provided critical contextual data for correlating vibration events with operational conditions.

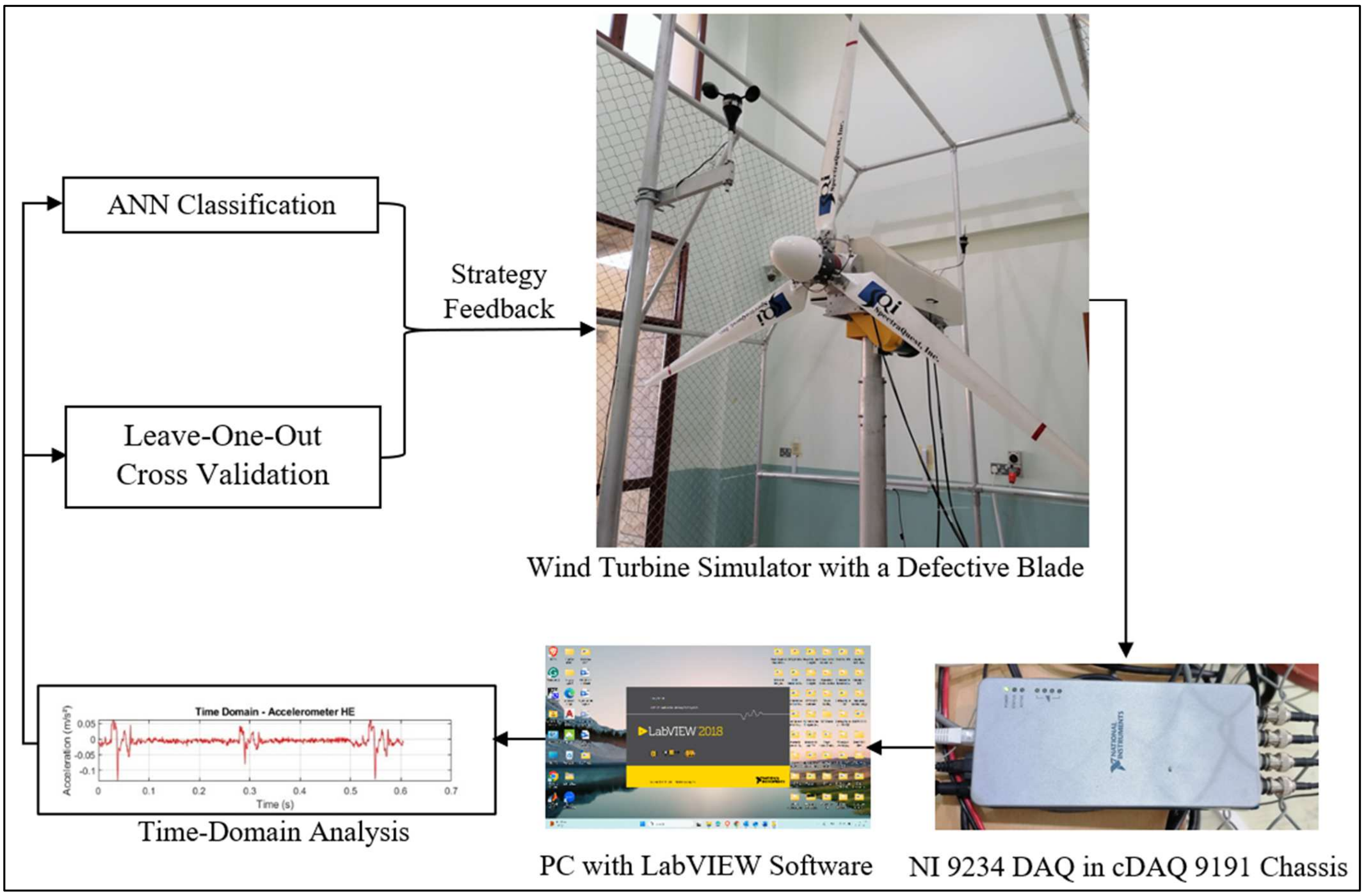

Fig. 1. Experimental schematic configuration of the setup.

Table 1. Details of sensors used in this study.

Sensor type and label	Location
Tachometer	Mounted to track shaft rotation speed in volts and rpm
Accelerometer (HE)	Mounted horizontally on the secondary bearing block along the east-facing axis
Accelerometer (HW)	Mounted horizontally on the secondary bearing block along the west-facing axis
Accelerometer (V)	Mounted vertically on the same bearing block

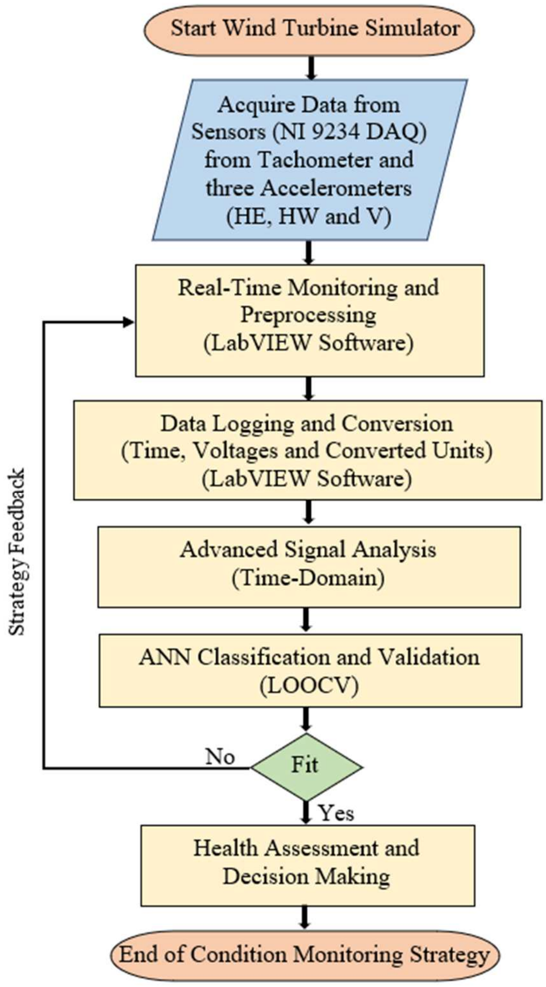

Fig. 2. Experimental flow chart.

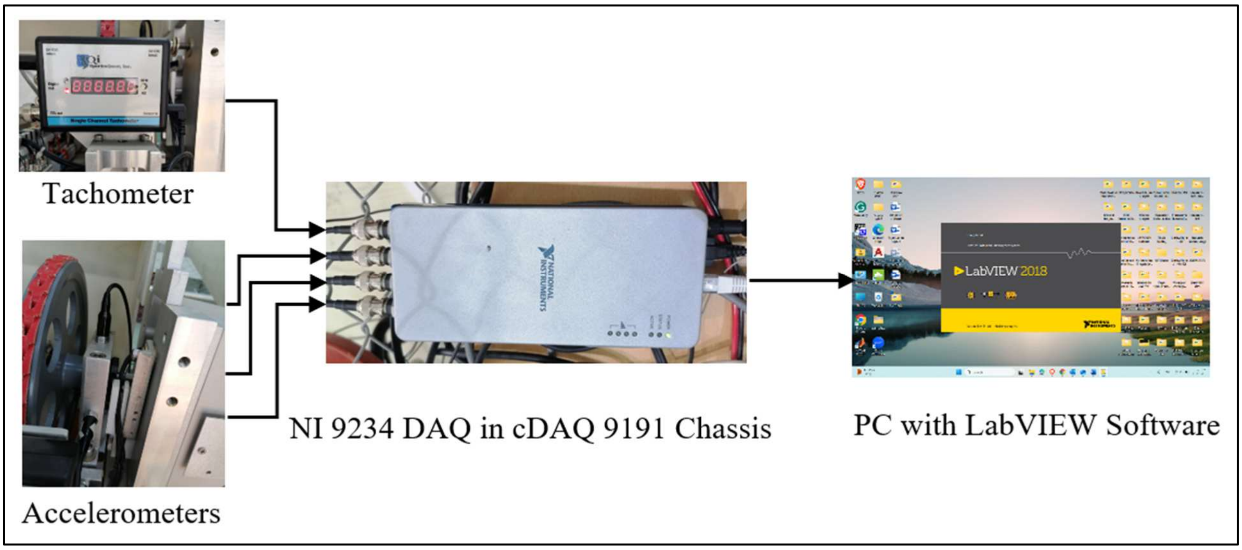

Fig. 3. Schematic representation of DAQ setup.

Table 2. Format of recorded parameters.

Parameter	Unit	Description
Time	s	Time stamp of each recorded data point
Tachometer Voltage	V	Raw voltage output from the tachometer
Tachometer rpm	rpm	Rotational speed of the turbine
Accelerometer (HE) Voltage	V	Raw signal from Horizontal East accelerometer
Accelerometer (HE) Acceleration	m/s²	Calibrated acceleration from HE sensor
Accelerometer (HW) Voltage	V	Raw signal from Horizontal West accelerometer
Accelerometer (HW) Acceleration	m/s²	Calibrated acceleration from HW sensor
Accelerometer (V) Voltage	V	Raw signal from Vertical accelerometer
Accelerometer (V) Acceleration	m/s²	Calibrated acceleration from V sensor

The raw voltage outputs from the tachometer and accelerometers were preprocessed in the LabVIEW. The preprocessing stage involved two key operations: signal filtering and unit conversion. The voltage signals from accelerometers were translated into acceleration (m/s²) using calibration constants shown in Fig. 4. Similarly, the tachometer output was converted from voltage to revolutions per minute (rpm) using a linear calibration factor derived from known reference speeds. The noise reduction was achieved through low-pass filtering, which helps in eliminating high-frequency components that do not contribute to fault diagnosis but can distort statistical features. The preprocessed signals were exported to structured data output file containing timestamped data columns for HE, HW and V acceleration, as well as the rotational speeds. This standardized format is shown in Table 2. It ensured seamless integration with MATLAB for further analysis.

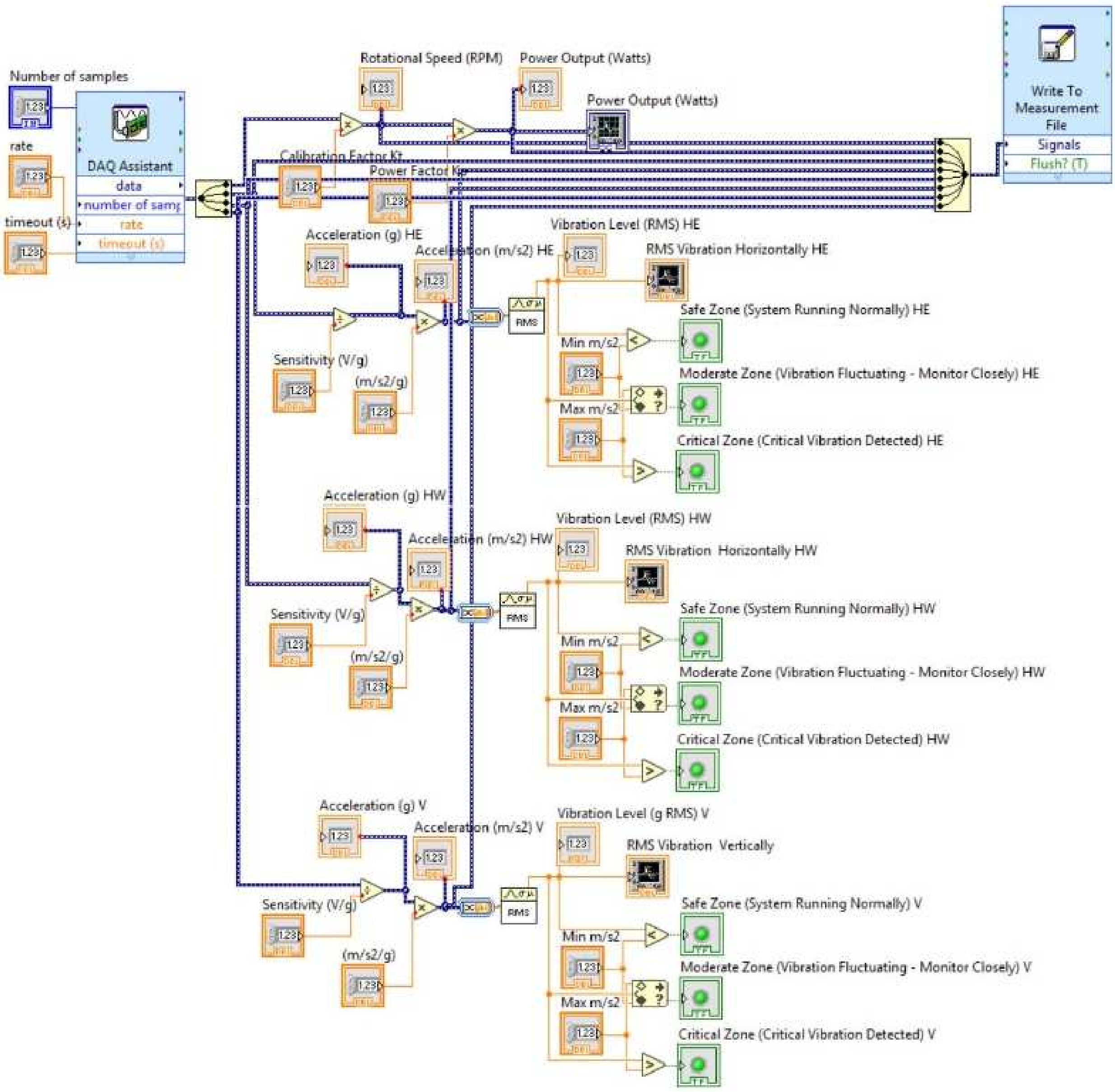

Fig. 4. LabVIEW block diagram representation.

Table 3. Details of extracted features.

Feature	Purpose
Root Mean Square (RMS)	Quantifies the energy content of the signal and is sensitive to changes in overall vibration intensity
Peak Acceleration	Identifies the maximum value in the signal, which indicates sudden impacts or high-force events
Crest Factor	Defined as the ratio of the peak value to RMS, this metric is effective in highlighting transient spikes such as shocks or impacts
Shock Pulse Count	Counts the number of acceleration values exceeding ±3 standard deviations from the mean (3σ method), offering a robust indicator of impulsive events likely caused by structural defects

To enhance the diagnostic reliability, additional data processing steps were implemented before the feature extraction. The raw accelerometer signals were detrended and normalized to eliminate the baseline drift and amplitude the bias between channels. A Butterworth low-pass filter was applied to suppress the high-frequency electrical noise while preserving the mechanical vibration content associated with stiffness variation and crack-induced impacts. Each signal was then standardized in MATLAB for cross-comparison among the given three sensor orientations. The comparative visualization of time-series signals and histograms showed the clear observation of vibration intensity shifts and transient spikes. This is which correspond to stiffness variations due to developing cracks. This could improve the visualization and clarify the relationship between time-domain features (RMS, crest factor and shock pulse count) and the mechanical condition of the turbine structure.

The time-domain analysis provides an intuitive and computationally efficient way to characterize the vibration signals. It extracted the statistical descriptors from raw acceleration signals which reflect underlying mechanical behaviours. The MATLAB scripts were developed to process the experimental data and compute the following features for each of the three sensor directions as listed in Table 3. Each feature was computed independently for HE, HW and V axes. This produced a total of nine features per sample. The visualizations such as time-series plots and histograms were also generated to inspect the feature distributions and detect anomalies. The labelling scheme consisted of three categories, namely: healthy, blade imbalance and blade crack. This annotation ensured the availability of ground truth labels for the supervised learning. The labels were stored in MATLAB-compatible categorical formats to facilitate the direct use in machine learning model training.

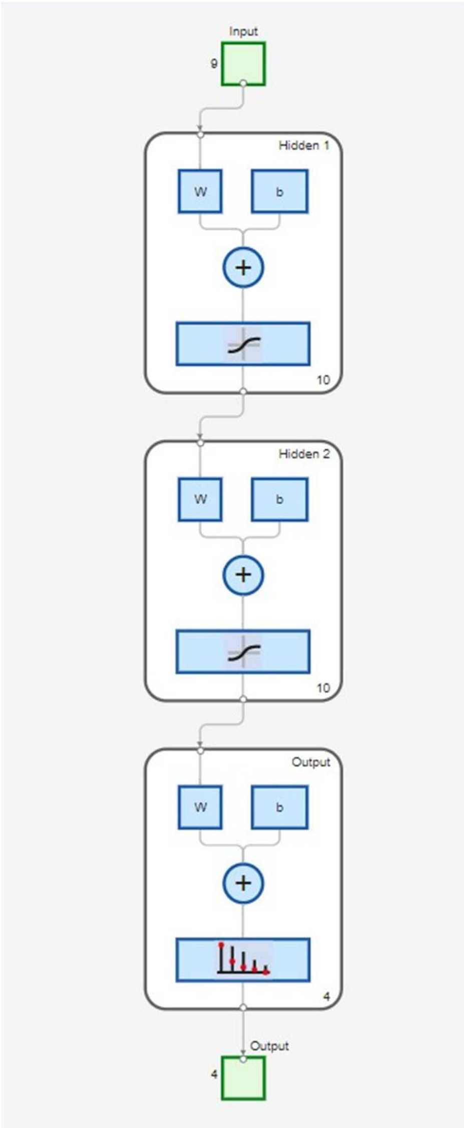

Fig. 5. ANN Architecture.

In this study, the vibration signals were obtained under the healthy operating condition, they were designated as the reference baseline for comparative analysis. All fault-state signals were evaluated relative to this reference to quantify deviations in vibration amplitude, crest factor and transient activity. Such reference-based comparison enabled the identification of stiffness-related changes in the turbine structure caused by blade cracks or imbalance. The use of experimentally measured reference data aligns with structural monitoring practices where baseline datasets are essential for reliable fault detection.

A multilayer feedforward ANN was implemented using MATLAB's patternnet function. The network architecture, shown in Fig. 5, comprised an input layer with 9 neurons corresponding to the extracted time-domain features, two hidden layers, each containing 10 neurons with sigmoid activation functions and an output layer with 4 neurons representing the fault classes: bearing fault, blade crack, blade imbalance and healthy.

The training algorithm employed backpropagation with Levenberg-Marquardt optimization. The small dataset size necessitated a strong validation strategy to ensure the generalizability. Hence, the LOOCV technique was adopted. In this LOOCV, each sample was held out in turn as a test case while the remaining samples were used to train the model. This procedure was repeated such that each sample was tested exactly once. This ensured a maximum data utilization while minimizing the risk of overfitting. The model performance was assessed using standard classification metrics. This included confusion matrix for a visual summary of classification results and F1-Score for a balanced performance measure. The MATLAB scripts generated these metrics for both full dataset training and LOOCV results.

3. Results and Discussion

The time-domain vibration features were extracted from the WTS under the three different operating conditions; healthy, blade crack and blade imbalance. The analysis was conducted across three sensor orientations; Horizontal East (HE), Horizontal West (HW) and Vertical (V). For each direction, four key statistical features were computed; Root Mean Square (RMS), Peak Acceleration, Crest Factor and Shock Pulse Count. These features were used to evaluate the sensitivity of each axis in detecting faults, then followed by classification results using an ANN.

3.1. Horizontal East (HE) axis analysis

The HE axis proved to be the most diagnostically informative among all three orientations. The HE sensor recorded an RMS acceleration of 0.0162 m/s^2, a peak acceleration of 0.1310 m/s^2 and a crest factor of 8.104. This indicated a significant transient activity and energy content. A total of 18 shock pulses were detected using the $\pm 3\sigma$ statistical threshold method, with a concentration of shocks observed in the 0.17s to 0.20s time window. These transients corresponded to sudden impacts or structural anomalies such as blade cracks.

Figure 6 shows the time-domain vibration signal from the HE sensor. This clearly marked the detected shock pulses exceeding the threshold range. The time-series plot was visually enriched with $\pm 3\sigma$ boundaries. This highlighted the abnormal spikes indicative of the mechanical faults. Figure 7 presents the corresponding histogram of acceleration values. It reveals a skewed distribution centered around -0.02 m/s^2. It has a long tail of high-magnitude outliers since it is typically experiencing fault-induced vibrations. The histogram validates the presence of significant deviations from normal operation.

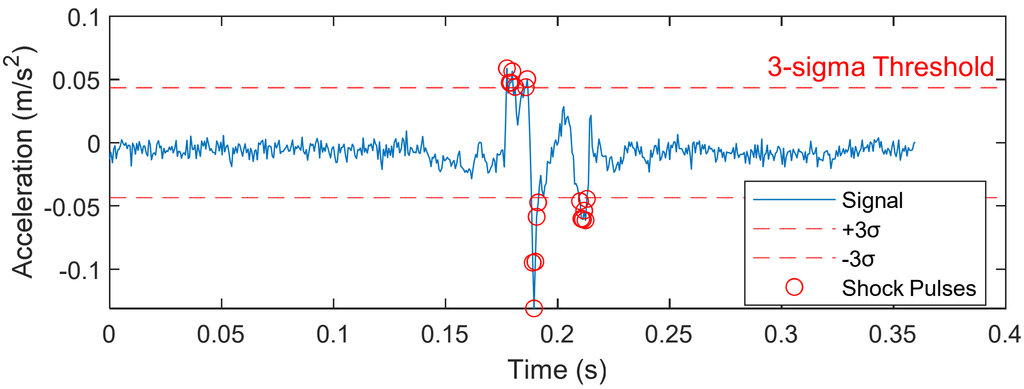

Fig. 6. Time-domain vibration signal (HE axis) after preprocessing and filtering showing detected shock pulses ($\pm 3\sigma$) associated with stiffness variation due to cracks.

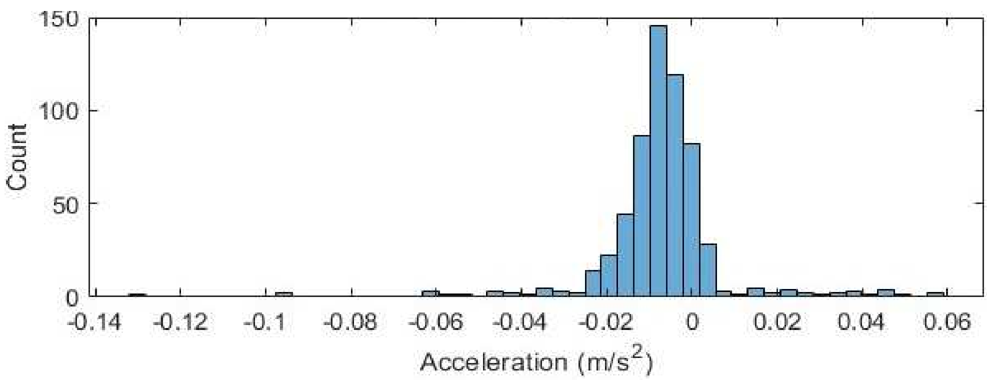

Fig. 7. Histogram of HE-axis acceleration data highlighting skewness and outliers representing transient stiffness changes in the turbine structure.

3.2. Horizontal West (HW) axis analysis

The HW sensor recorded less intense vibrations, with an RMS acceleration of 0.0065 m/s², a peak acceleration of 0.0168 m/s² and a crest factor of 2.6082. The shock pulse count was 19. However, these events were more evenly distributed and lacked distinct clustering and made them less diagnostically useful. Figure 8 illustrates the HW time-domain signal. It appeared noisier with fewer prominent transients. The shock pulses detected are scattered throughout the signal duration. This suggested either random noise or minor structural disturbances. Figure 9 shows the HW histogram with a broader and more symmetric distribution centered around -0.005 m/s². This signal structure lacks the skewness and kurtosis seen in fault-dominant axes like HE.

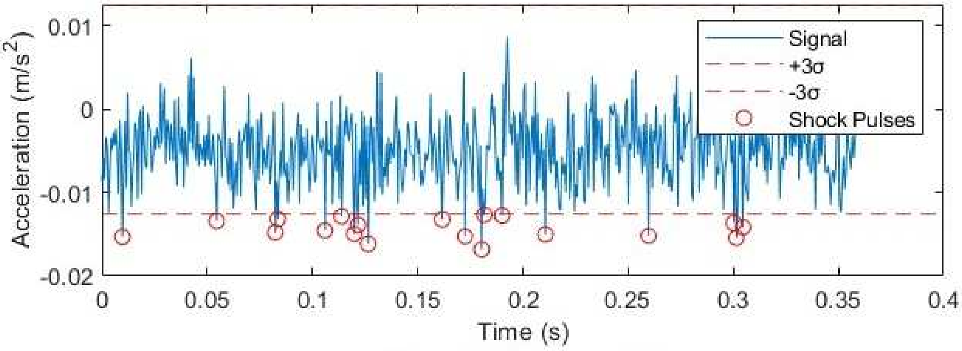

Fig. 8. Time-domain vibration signal measured along the Horizontal-West (HW) axis after preprocessing and ±3σ shock-pulse detection.

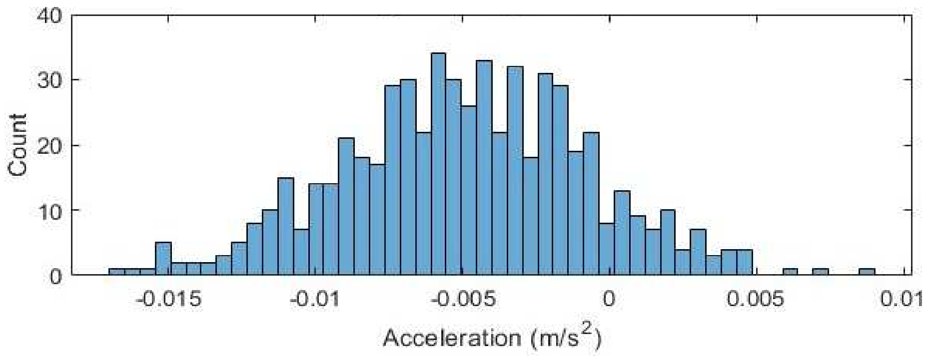

Fig. 9. Histogram of HW-axis acceleration data illustrating a broad, nearly symmetric distribution centered around –0.005 m/s².

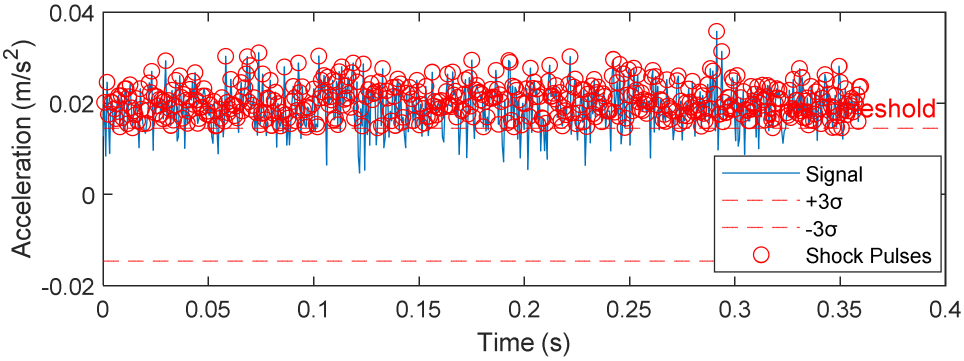

Fig. 10. Time-domain vibration signal acquired from the Vertical (V) axis after filtering and ±3σ thresholding for shock-pulse identification.

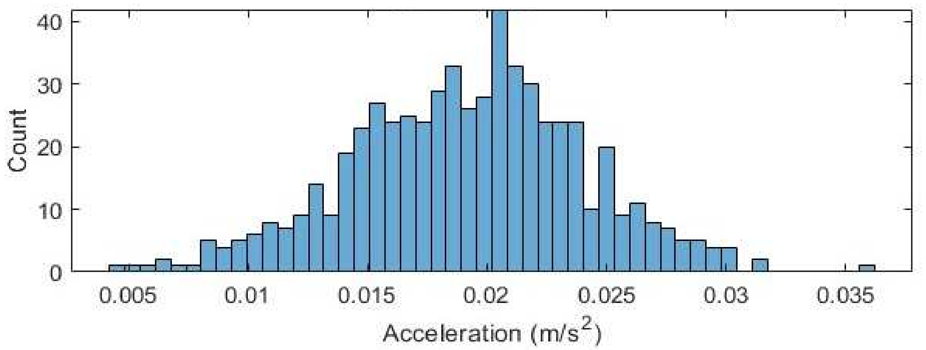

Fig. 11. Histogram of vertical-axis acceleration values showing a near-Gaussian distribution centered around 0.02 m/s².

Table 4. Comparative vibration metrics and diagnostic insights.

Metric	HE	HW	V
RMS (m/s²)	0.0162	0.0065	0.0198
Peak Acceleration (m/s²)	0.1310	0.0168	0.0358
Crest Factor	8.104	2.6082	1.8106
Shock Pulse Count	18	19	497

Table 5. ANN Confusion Matrix.

	Predicted: Crack	Predicted: Imbalance	Predicted: Healthy
Actual: Crack	2	0	0
Actual: Imbalance	0	2	0
Actual: Healthy	0	0	2

Table 6. ANN Classification Performance.

Class	Precision	Recall	F1-Score
Blade Crack	1.00	1.00	1.00
Blade Imbalance	1.00	1.00	1.00
Healthy	1.00	1.00	1.00

3.3. Vertical (V) axis analysis

Despite recording the highest number of shock pulses (497), the vertical axis data exhibited characteristics of structural or ambient noise rather than fault-specific indicators. The extracted features were RMS of 0.0198 m/s², peak acceleration was 0.0358 m/s² and crest factor was the lowest at 1.8106. As shown in Fig. 10, the time-domain signal comprised many low-amplitude spikes evenly distributed throughout the time duration. These patterns were not consistent with mechanical impacts like cracks or imbalance. Figure 11 presents a histogram with a near-Gaussian distribution centered around 0.02 m/s². This reflects structural oscillations and lacks extreme outliers.

3.4. Comparative vibration metric summary

Table 4 summarizes the diagnostic effectiveness of the vibration sensors in three directions. The vertical direction exhibits the highest RMS value and shock pulse count. This indicated greater sensitivity to vibration and impact events. The HE direction shows the highest crest factor and peak acceleration. This showed that it is more responsive to transient shock events. In contrast, The HW direction recorded the lowest values across most metrics. This indicated a limited diagnostic sensitivity. The V direction demonstrates superior fault detection capability, while the HE direction gave valuable visions into impulsive or shock-related anomalies.

3.5. ANN classification results

The ANN-based classification was applied to the fully labelled dataset without any training-testing split and achieved perfect performance. This was reflected in the confusion matrix and shown in Fig. 12. All samples were correctly classified across the four classes; Class1: bearing fault, Class 2: blade crack, Class 3: blade imbalance and Class 4: healthy. The combined confusion matrix aggregated the training, validation and test data to present a holistic view of the ANN model's performance. The matrix confirmed that the model correctly classified all seven available samples across the four classes and resulted in an overall accuracy of 100%. The class-wise breakdown revealed correct classification for one sample in Class 1 (14.3%), two in Class 2 (28.6%), two in Class 3 (28.6%) and two in Class 4 (28.6%). However, class 1 has only one sample and this could cause an error. At least 2 samples per class were needed for a valid train-test split. Hence, class 1 could be removed from training the ANN model. Table 5 and Table 6 represent the performance evaluation of the ANN classifier trained on time-domain vibration features for fault detection in wind turbines.

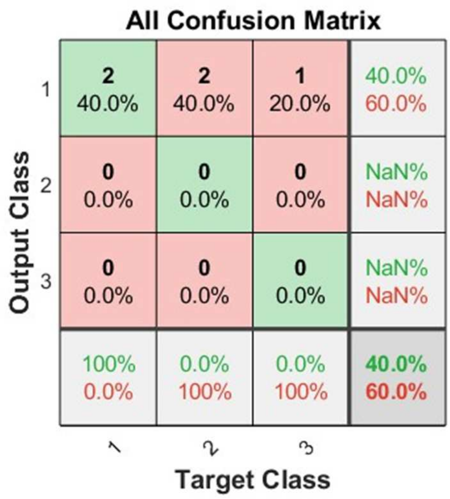

Fig. 12. Confusion matrix of ANN classification results showing perfect prediction across all classes, indicating strong separation among the four classes

Table 7. LOOCV Confusion Matrix.

	Predicted: Crack	Predicted: Imbalance	Predicted: Healthy
Actual: Crack	2	0	0
Actual: Imbalance	1	1	0
Actual: Healthy	0	0	2

Table 8. LOOCV Classification Performance.

Class	Precision	Recall	F1-Score
Blade Crack	0.67	1.00	0.80
Blade Imbalance	1.00	0.50	0.67
Healthy	1.00	1.00	1.00

Table 9. Summary of differences between ANN and LOOCV Confusion Matrices.

Feature	ANN Confusion Matrix	LOOCV Confusion Matrix
Evaluation Method	Likely standard test or train	Leave-One-Out Cross-Validation
Total Samples	6	6
Correct Predictions	6/6 (100%)	5/6 (~83.3%)
Misclassifications	0	1 (Imbalance shows crack)
Realism of Result	Possibly optimistic	More realistic
Overfitting Check	May not detect it	Helps detect overfitting

Table 10. Main differences between ANN and LOOCV classification reports.

Metric	ANN classification report	LOOCV classification report
Evaluation	Likely on training/test split	LOOCV (robust)
Performance	Perfect (1.00 for all)	Realistic with small errors
Precision	1.00 for all classes	Lower for Crack (0.67)
Recall	1.00 for all classes	Lower for Imbalance (0.50)
F1-Score	1.00	0.67–1.00 depending on class
Realism	Possibly optimistic	Realistic for small data

Using LOOCV on the labelled dataset, the ANN model achieved an overall accuracy of 83.3%, correctly classifying 5 out of 6 samples. As shown in Tables 7 and 8, the confusion matrix revealed perfect classification for the blade crack and healthy classes, while one blade imbalance sample was misclassified as blade crack. The classification report indicated that blade crack and healthy classes had high recall and F1-scores, whereas blade imbalance showed the lower recall at 0.50 and an F1-score of 0.67. Although the dataset was small, the LOOCV provided a more reliable and unbiased estimate of the model's performance compared to evaluation on the full dataset.

The difference between the Confusion Matrices lies in the classification performance of the model under two different conditions or evaluation methods. Table 5 shows the ANN Confusion Matrix. This was likely the result of evaluating an ANN on a training or test set and possibly with a standard train/test split. The matrix showed the perfect classification as all 6 samples were correctly predicted. It showed also no misclassifications. This indicated a well-trained model or potential overfitting if evaluated on training data. Table 7 shows the LOOCV Confusion Matrix. This resulted from the more strong and stringent validation LOOCV technique. The matrix showed one imbalance sample that was incorrectly predicted as Crack. It showed also one misclassification out of 6 total samples. This demonstrated slightly reduced accuracy under cross-validation and was is expected to be more realistic. Table 9 shows the summary differences between them.

The classification performance lies in the model under different evaluation strategies. Table 6 shows the ANN classification performance. This corresponded to Table 7's confusion matrix where the model made no mistakes. It showed a perfect classification and indicated 100% performance for all classes. It likely evaluated on the same data used for training or a very favourable test set. This could propose overfitting especially with a small dataset and could also show ideal model performance on possibly seen or well-partitioned data. Table 10 shows the LOOCV Classification Report. This corresponded to Table 7's confusion matrix using the LOOCV. It showed a more realistic performance due to LOOCV with one misclassification as one imbalance sample was predicted as Crack.

This result showed that the blade crack has lower precision (only 2 predicted as crack, but 1 was a false positive). Also, it showed that the blade imbalance has lower recall (only 1 out of 2 imbalance samples was correctly classified). Table 8 uses the LOOCV technique which revealed how well the model generalizes to unseen data. The LOOCV results were more trustworthy to prevent overfitting. Table 10 shows the main differences between ANN and LOOCV classification reports.

The achieved LOOCV classification accuracy of 83.3 % demonstrated that the proposed ANN model provided a competitive performance when compared with existing machine-learning-based fault detection studies. Hasan et al. [17] employed hybrid feature extraction combining time and frequency domains and entropy-domain parameters for fault detection. They reported an accuracy of 88 % though at a higher computational cost. Parziale et al. [18] used convolutional neural networks integrated with autoencoders for vibration-based fault diagnosis. They achieved 94–97 % accuracy but required high-level processing. Similarly, Al-Saad et al. [21] implemented the time-domain statistical features with an ANN classifier for rotary machines and achieved about 85–90 % accuracy. In contrast, the present study's lightweighted ANN and relied solely on four easily computed time-domain features. It achieved a comparable accuracy using minimal data and without frequency-domain transformations. This highlighted the method's suitability for real-time, resource-efficient condition monitoring of wind turbine systems.

This comparative framework highlights the potential integration of computational models, such as finite element simulations, as corresponding reference data to strengthen the structural interpretation and enhance the diagnostic accuracy. Consistent with existing literature, the findings reaffirm that time-domain vibration features combined with neural network-based classification can effectively identify early-stage blade and component faults in wind turbines [23, 24]. Prior studies have reported the classification accuracies of up to 97% using similar approaches where statistical time-domain features were extracted from the vibration signals and analyzed through classifiers such as k-nearest neighbours or convolutional neural networks [25, 26]. While these methodologies demonstrate high potential for real-time fault detection, continued refinement and validation across varying turbine configurations are essential to ensure generalized, robust, and scalable condition monitoring performance.

3.6. Synthesis of final results

The comprehensive analysis of the time-domain vibration data and machine learning-based classification yielded several critical understandings. Firstly, the HE axis consistently demonstrated the highest diagnostic sensitivity. It exhibited the greatest crest factor and most prominent transient indicators. Thereby, validating its selection as the primary channel for fault detection. Secondly, the ANN model was structured with nine input features derived solely from time-domain metrics. It achieved an overall classification accuracy exceeding 83% under LOOCV. This confirmed the suitability of using time-domain features alone for reliable fault classification. Lastly, the extracted time-domain features effectively discriminated between all examined operational states with especially clear separation observed between blade crack and healthy conditions. This reinforced the diagnostic strength of the proposed methodology.

4. Conclusions

This research established a comprehensive and low-complexity methodology for fault detection in wind turbine systems using exclusively time-domain vibration features combined with Artificial Neural Network (ANN) classification. The study involved experimental data acquisition from a lab-scale WTS equipped with tri-axial accelerometers mounted on the secondary bearing block in HE, HW and V orientations. The vibration signals were captured through a National Instruments NI 9234 DAQ system interfaced with LabVIEW which converted the signals from voltage to calibrated acceleration values. The data from each axis was subjected to time-domain feature extraction in MATLAB with more focusing on four computationally efficient metrics: RMS, Peak Acceleration, Crest Factor and Shock Pulse Count. These features were extracted independently from each of the three sensor directions and formed nine-dimensional feature vectors used as inputs to a feedforward ANN model. The ANN was constructed with two hidden layers and trained using the Levenberg–Marquardt algorithm. It was evaluated under both standard and Leave-One-Out Cross-Validation (LOOCV) conditions. The results showed that the HE axis provided the most diagnostically rich signal with a high crest factor (8.104) and peak acceleration (0.131 m/s^2). This made it the optimal axis for detecting blade-related anomalies. In contrast, the HW and V axes displayed lower signal clarity and were less effective in fault distinction. The classification results from the ANN demonstrated 100% accuracy on the training dataset and 83.3% under LOOCV with perfect recall for blade crack and healthy classes and moderate recall of 50% for blade imbalance. This variation highlighted the strong discriminative capacity of time-domain features for dominant fault conditions. However, additional feature engineering or sensor fusion may be required to improve sensitivity to subtler anomalies. The study confirmed the sufficiency of time-domain vibration features for fault classification and reduced the need for computationally intensive frequency-domain analyses. Future extensions of this work might incorporate computational reference models, such as finite element-based structural simulations, to balance the experimentally measured baseline data. This integration will enhance the interpretation of the vibration responses by linking the measured dynamics with theoretical stiffness and modal variations. Thereby, they are reinforcing the mechanical foundation of the fault detection framework. To enhance the robustness of the proposed framework, the future work should integrate computational structural analysis with experimental measurements. Finite element or modal simulations can be used to model stiffness variations and crack-induced dynamic behavior. This could provide reference parameters such as natural frequencies and stress distributions. This work advanced the practical implementation of intelligent condition monitoring systems in wind energy applications by validating the effectiveness of lightweight ANN models using minimal datasets. It also paved the way for future work exploring the sensor fusion, ensemble learning and microcontroller-based deployment. This could enhance the scalability and field-readiness for predictive maintenance in sustainable energy infrastructures.

Author Contributions

A.H. Al-Hinai designed the framework of this research paper and was a major contributor to writing the manuscript. K.C. Varaprasad was a major contributor in revising and improving sections 1 and 2. V. Vinod Kumar was also a major contributor to revising the manuscript and improving sections 3 and 4. All authors discussed the results, reviewed and approved the final version of the manuscript.

Acknowledgments

The authors are thankful to the Faculty of Engineering at Sohar University for their guidance and cooperation.

Conflict of Interest

The authors declared no potential conflicts of interest concerning the research, authorship and publication of this article.

Funding

The authors received no financial support for the research, authorship, and publication of this article.

Data Availability Statements

The datasets generated and/or analyzed during the current study are available from the corresponding author on reasonable request.

Nomenclature

ANN	Artificial Neural Networks	RMS	Root Mean Square
CMS	Condition Monitoring Systems	VA	Vibration Analysis
DAQ	Data Acquisition System	WTS	Wind Turbine Simulator
LOOCV	Leave-One-Out Cross-Validation		

References

[1] Al-Hinai, A. H., Varaprasad, K. C., Kumar, V. V., Comprehensive review of vibration-based analysis for wind turbine condition monitoring, *Mechanical Engineering for Society and Industry*, 4(3), 2024, 570–605.
[2] Swadi, M., Kadhim, D. J., Salem, M., Tuaimah, F. M., Majeed, A. S., Alrubaie, A. J., Investigating and predicting the role of photovoltaic, wind and hydrogen energies in sustainable global energy evolution, *Global Energy Interconnection*, 7(4), 2024, 429–445.
[3] Chen, R., Qin, D., Liu, C., Dynamic modelling and dynamic characteristics of wind turbine transmission gearbox-generator system electromechanical-rigid-flexible coupling, *Alexandria Engineering Journal*, 65, 2022, 307–325.
[4] Ozturkoglu, O., Ozcelik, O., Günel, S., Effects of operational and environmental conditions on estimated dynamic characteristics of a large in-service wind turbine, *Journal of Vibration Engineering and Technologies*, 12, 2024, 803–824.
[5] Li, Y., Zhu, C., Chen, X., Tan, J., Fatigue Reliability analysis of wind turbine drivetrain considering strength degradation and load sharing using survival signature and FTA, *Energies*, 13(8), 2020, 2108.
[6] Chang, C. C. W., Ding, T. J., Han, W., Chai, C. C., Bhuiyan, M. A. S., Choon-Yian, H., Song, T. C., Recent advancements in condition monitoring systems for wind turbines: A review, *Energy Reports*, 9, 2023, 22–27.
[7] Tritschler, N., Dugenske, A., Kurfess, T., An automated Edge Computing-Based condition health monitoring system: with an application on rolling element bearings, *Journal of Manufacturing Science and Engineering*, 143(7), 2021, 071006.
[8] Kumar, V., Dhami, S., Goyal, D., Intelligent Condition Monitoring Techniques for Early fault diagnosis of rotating Machines – a review, *Journal of University of Shanghai for Science and Technology*, 23(8), 2021, 549–566.
[9] Chavan, N. P., Kale, M. S., Deshmukh, S. P., Thakar, C. M., A review on development and trend of condition monitoring and fault diagnosis, *ECS Transactions*, 107(1), 2022, 17863–17870.
[10] Surucu, O., Gadsden, S. A., Yawney, J., Condition Monitoring using Machine Learning: A Review of Theory, Applications and Recent Advances, *Expert Systems with Applications*, 221, 2023, 119738.
[11] Cakir, M., Guvenc, M. A., Mistikoglu, S., The experimental application of popular machine learning algorithms on predictive maintenance and the design of IIoT based condition monitoring system, *Computers and Industrial Engineering*, 151, 2020, 106948.
[12] Al-Hinai, A. H., Varaprasad, K. C., Kumar, V. V., Performance optimization of a horizontal axis wind turbine simulator under the effects of blade's pitch angle variation, *Research on Engineering Structures and Materials*, 11(5), 2025, 2331-2349.
[13] Narasinh, V., Mital, P., Chakravortty, N., Mittal, S., Kumar, A. V., Venkatraman, C., Kulkarni, N., Thakur, I., Analysing and Forecasting Degradation in Wind Turbines under Transient Operating Conditions through Vibration Analysis, *E3S Web of Conferences*, 572, 2024, 01006.
[14] Patil, H., Patel, D., Diagnosis of localized defects in floating bush bearings through time-frequency domain analysis, *Maintenance Reliability and Condition Monitoring*, 3(2), 2023, 27–44.
[15] Charan, K. S., An Auto-Encoder based TinyML approach for Real-Time anomaly detection, *SAE International Journal of Advances and Current Practices in Mobility*, 5(4), 2022, 1496–1501.
[16] Aasi, A., Tabatabaei, R., Aasi, E., Jafari, S. M., Experimental investigation on time-domain features in the diagnosis of rolling element bearings by acoustic emission, *Journal of Vibration and Control*, 28(19–20), 2021, 2585–2595.
[17] Hasan, M. J., Rashid, M., Nasir, A. F. A., Abdullah, M. A., Razman, M. A. M., Musa, R. M., Majeed, A. P. P. A., Gearbox Fault Diagnostics: an examination on the efficacy of different feature extraction techniques, *Advances in Intelligent Systems and Computing,* 2021, 399–406.
[18] Parziale, M., Lomazzi, L., Giglio, M., Cadini, F., Vibration-based structural health monitoring exploiting a combination of convolutional neural networks and autoencoders for temperature effects neutralization, *Structural Control and Health Monitoring*, 29(11), 2022, 3076.
[19] Kulevome, D. K. B., Wang, H., Wang, X., Deep Neural Network based Classification of Rolling Element Bearings and Health Degradation Through Comprehensive Vibration Signal Analysis, *Journal of Systems Engineering and Electronics*, 33(1), 2022, 233–246.
[20] Moghadam, A., Kakhki, F., *Comparative Study of Decision Tree Models for Bearing Fault Detection and Classification*, In: Tareq Ahram, Waldemar Karwowski, Pepetto Di Bucchianico, Redha Taiar, Luca Casarotto and Pietro Costa (eds) Intelligent Human Systems Integration (IHSI 2022): Integrating People and Intelligent Systems, AHFE (2022) International Conference, Vol. 22, AHFE International, USA, 2022.
[21] Al-Saad, M., Al-Mosallam, M., Alsahlani, A. A. M., Best Time Domain features for early detection of faults in rotary machines using RAT and ANN, *Journal of Vibration Engineering and Technologies*, 11(3), 2022, 1137–1149.
[22] Alzghoul, A., Jarndal, A., Alsyouf, I., Bingamil, A. A., Ali, M. A., AlBaiti, S., On the Usefulness of Pre-processing Methods in Rotating Machines Faults Classification using Artificial Neural Network, *Journal of Applied and Computational Mechanics*, 7(1), 2021, 254-261.
[23] Rangel-Rodriguez, A. H., Machorro-Lopez, J. M., Granados-Lieberman, D., De Santiago-Perez, J. J., Amezquita-Sanchez, J. P., Valtierra-Rodriguez, M., Detection of Cracks in Low-Power Wind Turbines Using Vibration Signal Analysis with Empirical Mode Decomposition and Convolutional Neural Networks, AI, 6(8), 2025, 179.
[24] Bougoffa, M., Benmoussa, S., Djeziri, M., Contaret, T., Wind turbine blades fault diagnosis based on vibration signals utilizing convolutional neural network, *International Conference on Decision Aid Sciences and Applications (DASA)*, 2024, 1–5.
[25] Ali, W., El-Thalji, I., Giljarhus, K. E. T., Delimitis, A., Classification Analytics for wind turbine blade faults: Integrated Signal analysis and Machine learning approach, *Energies*, 17(23), 2024, 5856.
[26] Meyer, A., Vibration fault diagnosis in wind turbines based on automated feature learning, *Energies*, 15(4), 2022, 1514.

ORCID iD

Abdulhamid Hamdan Al-Hinai https://orcid.org/0009-0005-5354-2895
Karu Clement Varaprasad https://orcid.org/0000-0002-8182-804X
Viswanadhan Vinod Kumar https://orcid.org/0000-0001-5420-4584

How to cite this article: Al-Hinai A.H., Varaprasad K.C., Kumar V.V. Fault Detection in Wind Turbine Using Time-Domain Vibration Features and LOOCV-Tuned Neural Networks, *J. Appl. Comput. Mech.*, xx(x), 2025, 1–11.
https://doi.org/10.22055/jacm.2025.48637.5384